

Preparation and properties of Nd,Yb:GGG polycrystalline nanopowders

Yanmin DONG, Jing SUN*, Wensheng YU, Weihang LI, Fei TENG

School of Chemistry and Environmental Engineering, Changchun University of Science and Technology, Changchun 130022, China

Received: September 26, 2012; Revised: November 29, 2012; Accepted: December 1, 2012

©The Author(s) 2012. This article is published with open access at Springerlink.com

Abstract: Gadolinium gallium garnet (GGG) polycrystalline powders doped with Nd,Yb were prepared by co-precipitation method. The structure, phase and properties of powders were characterized by X-ray diffraction (XRD), Fourier transform infrared spectroscopy (FTIR), scanning electron microscope (SEM), energy dispersive X-ray spectroscopy (EDS) and fluorescence spectroscopy. XRD analysis indicated that the crystallization of Nd,Yb:GGG powders occur at 900 °C. SEM analysis showed that the morphology of the powders was irregular and the average radius is 68.74 nm. FTIR analysis manifested that pure Nd,Yb:GGG powders were formed at 900 °C. The fluorescence spectrum revealed that the most strong emission of Nd,Yb:GGG powders was 1030 nm, which was attributed to ${}^2F_{5/2} \rightarrow {}^2F_{7/2}$ of Yb^{3+} . The possible formation mechanism of Nd,Yb:GGG powders were preliminarily discussed.

Key words: Nd,Yb:GGG; co-precipitation method; fluorescence

1 Introduction

In the latest years, gadolinium gallium garnet (GGG) polycrystalline nanopowders have attracted great interest due to their high performance in technological applications [1-5]. Various methods have been explored to synthesize gadolinium gallium garnet (GGG) polycrystalline powders, such as solid-state method, sol-gel, hydrothermal method etc. However, the methods mentioned above had some disadvantages, such as the solid-state method required high temperature, the low productivity of the hydrothermal method and

the sol-gel method required expensive equipments. For liquid-phase co-precipitation method, the GGG polycrystalline powders with pure phase could be obtained in the lower sintered temperature and for shorter time (4 h), because the co-precipitation increased the activity of GGG synthesis reaction [6].

The ytterbium ion consisting only two energy levels: the ${}^2F_{5/2}$ excited state and the ${}^2F_{7/2}$ ground state, since the simplest energy level scheme, it is suited for diode pumping. In addition, the intense and broad Yb^{3+} absorption lines are well suited for infrared InGaAs diode laser pumping, the broad emission band allows the generation of ultra-short pulses and the small quantum defect between absorption and emission wavelengths, leads to a low thermal load [7,8]. The neodymium multiple excited states with high

* Corresponding author.
E-mail: sj-cust@126.com

absorption cross-section that it could be used for pulse pumping. The Nd-Yb energy transfer was very efficient because the system combine the Yb^{3+} good laser emission characteristics and the Nd^{3+} multiple excited states.

In this paper, Nd,Yb:GGG polycrystalline powders were fabricated by co-precipitation method. The morphology and luminescence characteristics of Nd,Yb:GGG polycrystalline powders and Nd \rightarrow Yb energy transfer were investigated.

2 Experimental details

2.1 Chemicals

The aqueous ammonia was purchased from Tianjin Tiantai Fine Chemical Reagents Co. Ltd. and HNO_3 was bought from Beijing Chemical Company. Yb_2O_3 (99.99 %), Ga_2O_3 (99.99 %), Nb_2O_3 and Gd_2O_3 were bought from Sinopharm Chemical Reagents Co. Ltd. $\text{Yb}(\text{NO}_3)_3$, $\text{Ga}(\text{NO}_3)_3$, $\text{Nb}(\text{NO}_3)_3$ and $\text{Gd}(\text{NO}_3)_3$ were prepared by dissolving Yb_2O_3 , Ga_2O_3 , Nb_2O_3 and Gd_2O_3 in dilute nitric acid, then the solution was heated to evaporate the water. All chemicals were of analytical grade and directly used as received without further purification.

2.2 Preparation of samples

Yb_2O_3 , Ga_2O_3 , Nb_2O_3 and Gd_2O_3 in a specific stoichiometric molar ratio were separately dissolved in nitric acid and the resulting solutions were mixed and stirred at room temperature. The resulting solution was slowly added dropwise into aqueous ammonia under constant stirring, keeping the pH around 9.0. The gelatinous white co-precipitate of gallium-gadolinium hydroxide with Nb,Yb was filtered, washed several times with distilled water to remove the residual nitrate ions, and finally oven dried at 60 °C to obtain the precursor powders. Selected portions were later calcination at 700 °C and 900 °C for 4 h in a muffle furnace under air atmosphere.

2.3 Characterization methods

X-ray powder diffraction (XRD) measurements were carried out on a MXP21VAHF diffractometer using CuK_α radiation with Ni filter ($\lambda=0.15405$ nm). The X-ray generator worked at a power of 40 kV and 40 mA. Fourier transform infrared spectroscopy (FTIR) was recorded on BRUKER Vertex 70. Fourier

transform infrared spectrometer was made by Germany Bruker Company with a resolution of 1 cm^{-1} , and the specimen for the measurement was prepared by mixing the sample with KBr powders. Then the mixture was pressed into pellets, and the spectrum was acquired in a wave number range from 4000 cm^{-1} to 400 cm^{-1} . Scanning electron microscope (SEM) images were taken with Jeol (Tokyo, Japan) JSM 5600. Samples were coated with a Au thin film, in order to avoid charging effects. The fluorescence measurements were performed on a Hitachi F-7000 spectrophotometer equipped with a 150 W argon lamp as the excitation source.

3 Results and discussion

3.1 XRD patterns

The X-ray diffraction patterns of Nd,Yb:GGG samples which were calcined at 700 °C and 900 °C were showed in Fig. 1. There was a broad peak around 32° for the composite powders, indicating that the samples were amorphous. However, when calcined after 900 °C, all the reflection peaks can be readily indexed to those of the pure cubic phase with primitive structure of GGG (PDF#13-0493), indicating that the pure phase of Nd,Yb:GGG polycrystalline powders was successfully prepared, its space group is I_a3d . Also, the structure of GGG was not changed when Nd^{3+} and Yb^{3+} were doped.

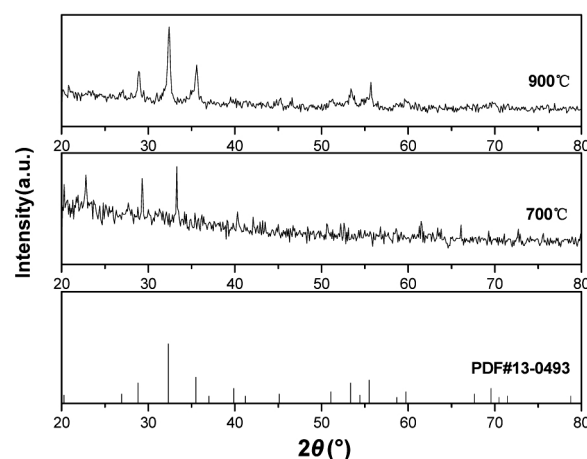
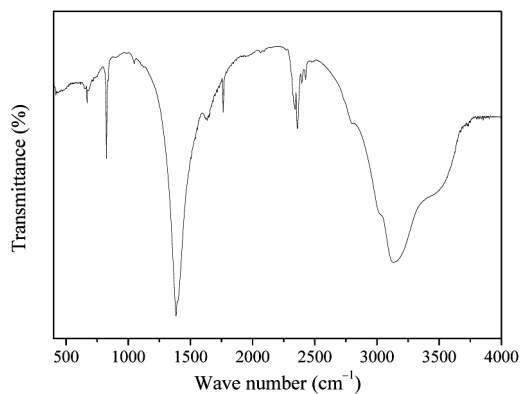


Fig. 1 XRD of Nd,Yb:GGG polycrystalline powders.

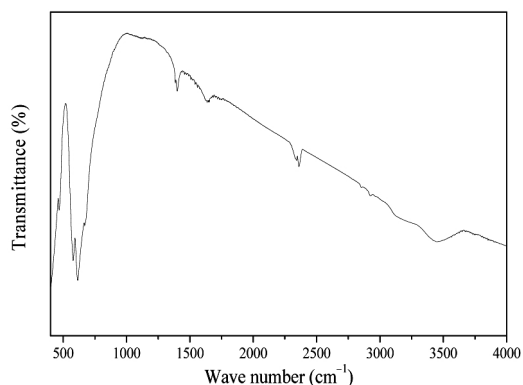
3.2 FTIR spectra analysis

Nd,Yb:GGG sample without calcination and the one

calcined at 900 °C were investigated by FTIR, as shown in Fig. 2. All the absorption peaks at about 3200-3700 cm^{-1} , corresponding to the stretching vibrations of hydroxyl group ($\nu_{\text{O-H}}$) and C-H bond ($\nu_{\text{C-H}}$), respectively. All the absorption peaks at about 1653 cm^{-1} and 1537 cm^{-1} were attributed to the combination of the carbonyl group ($\nu_{\text{C=O}}$), hydroxyl group ($\nu_{\text{O-H}}$) and C-H bond ($\nu_{\text{C-H}}$). All the absorption peaks weakened or disappeared and new absorption peaks appeared at low wave numbers after calcined at 900 °C (as shown in Fig. 2(b)). The peaks at 3467 cm^{-1} and 2367 cm^{-1} were attributed to the H_2O and CO_2 from ambient atmosphere. The weak peaks at 1644 cm^{-1} indicated that there was still a few of $-\text{NH}_2$ in the powders. The peaks at 1399 cm^{-1} were attributed to the stretching vibrations of few C-O bond ($\nu_{\text{C-O}}$) and C-C bond ($\nu_{\text{C-C}}$). The new peaks at 612 cm^{-1} and 464 cm^{-1} were associated with the metal-oxygen bonds (Gd-O and Gd-O-Ga) vibrations. FTIR analysis manifested that pure GGG polycrystalline powders



(a) The sample without calcination



(b) Nd,Yb:GGG polycrystalline powders calcined at 900 °C

Fig. 2 FTIR spectra of Nd,Yb:GGG polycrystalline powders.

were formed at 900 °C, and the peaks were sharp and obvious. The results were in good agreement with XRD patterns.

3.3 SEM analysis

Figure 3 showed the SEM images of Nd,Yb:GGG polycrystalline powders calcined at 900 °C. The morphology of the Nd,Yb:GGG samples was irregular agglomeration of small crystallites. Figure 4 showed the particle size distribution histograms of the Nd,Yb:GGG samples. The particle size distribution histograms showed the average diameter of the samples was 68.74 nm.

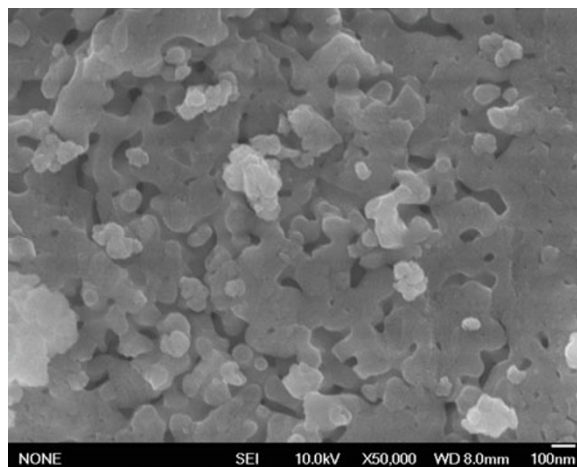


Fig. 3 SEM of Nd,Yb:GGG polycrystalline powders.

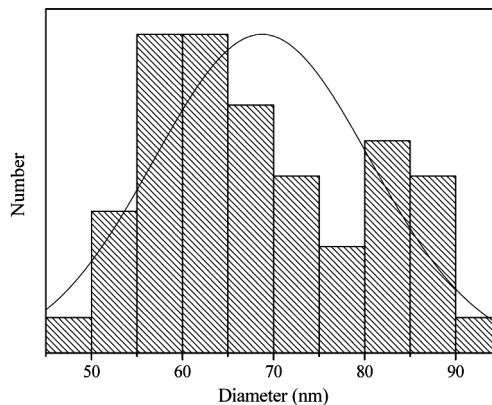


Fig. 4 Particle size distribution histograms.

3.4 EDS analysis

Figure 5 showed the EDS of Nd,Yb:GGG polycrystalline powders, demonstrating that the elements of Yb, O, Ga, Gd and Nd were existed in the powders.

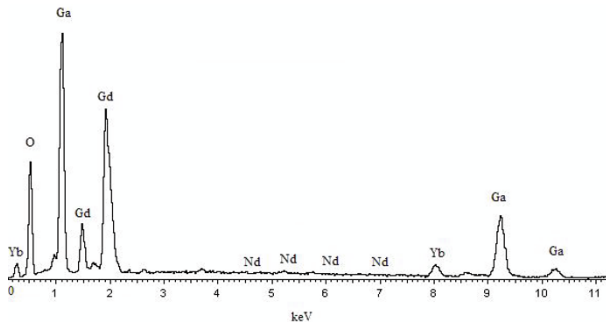


Fig. 5 EDS of Nd,Yb:GGG polycrystalline powders.

3.5 Photoluminescence properties

Figure 6 showed the fluorescence spectrum of Nd,Yb:GGG polycrystalline powders excited with argon ion laser at 488 nm. Between the waves at 900-1100 nm (the wavenumber was between 11 111.1 cm^{-1} and 9090.9 cm^{-1} showed in Fig. 6), there were two emission peaks with 977 nm (the wavenumber was 10 235.4 cm^{-1}) and 1030 nm (the wavenumber was 9708.7 cm^{-1}). The third one was at 1075 nm (the wavenumber was 9302.3 cm^{-1}). The strongest emission peak at 1030 nm was assigned to the ${}^2F_{5/2} \rightarrow {}^2F_{7/2}$ transition of Yb^{3+} . Analysis with the EDS, the Nd and Yb were exactly coexistence. However, Fig. 6 only showed the emission of Yb^{3+} , but the emission of Nd^{3+} was not showed. It indicated that in the process of emission, the Nd^{3+} gained energy and also transferred the energy to Yb^{3+} [9,10].

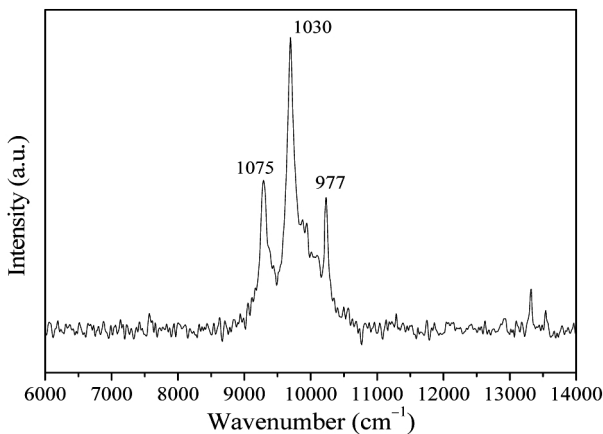


Fig. 6 Fluorescence spectrum of Nd,Yb:GGG polycrystalline powders.

3.6 The energy transfer of Nd,Yb

The Nd \rightarrow Yb energy transfer in GGG involves Nd $^{3+}$ (${}^4F_{3/2} \rightarrow {}^4I_{9/2}$) emission and Yb $^{3+}$ (${}^2F_{7/2} \rightarrow {}^2F_{5/2}$)

absorption. The large crystal field splittings of the levels assure the overlap of the Nd $^{3+}$ (${}^4F_{3/2} \rightarrow {}^4I_{9/2}$) emission with Yb $^{3+}$ (${}^2F_{7/2} \rightarrow {}^2F_{5/2}$) absorption. The resonant ET rates are proportional to the integral overlap of the experimental normalized line shapes

$$g(E) = \sigma(E) / \int \sigma(E) dE \frac{n!}{r!(n-r)!}$$

of the Nd $^{3+}$ emission

$$\text{and Yb}^{3+} \text{ absorption, } W \propto \int g_{\text{Nd}}^{\text{em}}(E) / g_{\text{Yb}}^{\text{abs}}(E) dE$$

[11]. Figure 7 showed the scheme of energy transfer for Nd $^{3+}$ and Yb $^{3+}$. The non-radiation energy transfer passed the energy to Yb $^{3+}$ through the transition of Nd $^{3+}$ from excited state to the ground state. The fluorescence emission was caused by the ${}^2F_{5/2} \rightarrow {}^2F_{7/2}$ radiation transition of Yb $^{3+}$. Because there is no overlap between Yb $^{3+}$ emission and Nd $^{3+}$ absorption, there is a very weak Yb \rightarrow Nd back transfer, implying the fluorescence emission of Nd $^{3+}$ is not reflected.

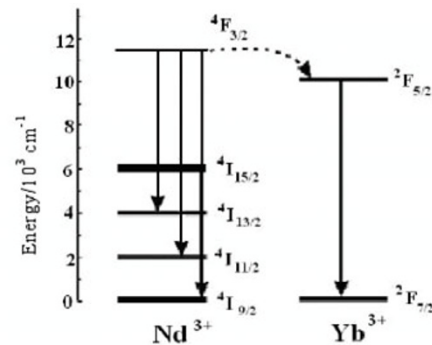


Fig. 7 Scheme of energy transfer for Nd $^{3+}$ and Yb $^{3+}$.

4 Conclusions

Nd,Yb:GGG polycrystalline powders have been successfully synthesized by co-precipitation method. After annealed at 900 $^{\circ}\text{C}$, the particles of the Nd,Yb:GGG polycrystalline powders showed an irregular shape and the average diameter was 68.74 nm. The fluorescence analysis revealed that the strongest emission peak (at 1030 nm) of Nd,Yb:GGG polycrystalline powders, which was attributed to the transition of ${}^2F_{5/2} \rightarrow {}^2F_{7/2}$ of Yb $^{3+}$.

References

- [1] Chenais S, Druon F, *et al.* Diode-pumped Yb:GGG laser: Comparison with Yb:YAG. *Optical Materials* 2003, **22**: 99-106.
- [2] Yoshida K, Yoshida H. Characterization of high

- average power Nd:GGG slab lasers. *IEEE Journal of Quantum Electronics* 1988, **24**: 1188-1192.
- [3] Lacovara PA, Choi HK, Wang CA, *et al.* Room-temperature diode-pumped Yb:YAG lasers. *Opt Lett* 1991, **16**: 1089-1091.
- [4] Belovolov MI, Dinao EM, Timoschechkin MI, *et al.* Room temperature Cw Yb:GGG laser operation at 1038-nm. *Conference on Lasers and Electro-optics Europe* 1996: 43.
- [5] Sun J, Zeng FM, Li JL, *et al.* Synthesis of Nd: GGG laser ceramics powder by sol-gel combustion method. *Journal of Synthetic Crystal* 2007, **4**: 935.
- [6] Zhao GJ, Li T, He XM, *et al.* Preparation of gadolinium gallium garnet polycrystalline material by coprecipitation method. *Materials Letters* 2002, **56**: 1098-1102.
- [7] DeLoach LD, Payne SA, Chase LL, *et al.* Evaluation of absorption and emission properties of Yb³⁺ doped crystals for laser applications. *IEEE Journal of Quantum Electronics* 1993, **29**: 1179-1191.
- [8] Baney DM, Rankin G, Chang KW. Simultaneous blue and green upconversion lasing in a laser-diode-pumped Pr³⁺/Yb³⁺ doped fluoride fiber laser. *Appl Phys Lett* 1996, **69**: 1662-1664.
- [9] Qiu HW, Yang PZ, Dong J, *et al.* The influence of Yb concentration on laser crystal Yb:YAG. *Materials Letters* 2002, **55**: 1-2.
- [10] Jiang BX, Zhao ZW, Xu XD, *et al.* Spectral properties and charge transfer luminescence of Yb³⁺:Gd₃Ga₅O₁₂ (Yb:GGG) crystal. *Journal of Crystal Growth* 2005, **277**: 186-191.
- [11] Dexter DL. A theory of sensitized luminescence in solids. *Chem Phys* 1953, **21**: 836.